

Dynamos, Super-pulsars and Gamma-ray bursts

Stephan Rosswog* and Enrico Ramirez-Ruiz†

**International University Bremen, Germany*

†*Institute for Advanced Study, Princeton, USA*

Abstract.

The remnant of a neutron star binary coalescence is expected to be temporarily stabilised against gravitational collapse by its differential rotation. We explore the possibility of dynamo activity in this remnant and assess the potential for powering a short-duration gamma-ray burst (GRB). We analyse our three-dimensional hydrodynamic simulations of neutron star mergers with respect to the flow pattern inside the remnant. If the central, newly formed super-massive neutron star remains stable for a good fraction of a second an efficient low-Rossby number $\alpha - \Omega$ -dynamo will amplify the initial seed magnetic fields exponentially. We expect that values close to equipartition field strength will be reached within several tens of milliseconds. Such a super-pulsar could power a GRB via a relativistic wind, with an associated spin-down time scale close to the typical duration of a short GRB. Similar mechanisms are expected to be operational in the surrounding torus formed from neutron star debris.

INTRODUCTION

While there is mounting evidence that the long-soft variety GRBs are related directly to the death of massive stars and go along with supernova explosions, there is so far little evidence about the progenitor of short-hard GRBs. The most popular candidates are binary coalescences of either a double neutron star or a stellar mass black hole with a neutron star. Most often a 'unified picture' for the GRB central engine, a new-born black hole plus a debris disk, is invoked. We will explore here the possibility that the central object of the merger remnant produces a GRB via magnetic processes *before* collapsing to a black hole. Further scenarios with ultra-magnetised neutron stars have been suggested, for example, by Usov (1992, 1994), Duncan and Thompson (1992), Thompson and Duncan (1994), Meszaroz and Rees (1997), Katz (1997) and Kluzniak and Ruderman (1998).

The merger of two neutron stars results in a massive central object, a thick, hot and dense torus of neutron star debris and some material on highly eccentric/unbound orbits [19, 20, 13]. The central object of the remnant is rapidly differentially rotating [12, 13, 4, 14] with rotational periods ranging from ~ 0.4 to ~ 2 ms [14]. Differential rotation is known to be very efficient in stabilising stars that are substantially more massive than their non-rotating maximum mass. For example, Ostriker and Bodenheimer (1968) constructed differentially rotating white dwarfs of $4.1 M_{\odot}$. A recent investigation analysing differentially rotating polytropic neutron stars [7] finds it possible to stabilise systems even beyond twice the typical neutron star mass of $2.8 M_{\odot}$. The exact time scale of this stabilisation is difficult to determine, as all the poorly known high-density

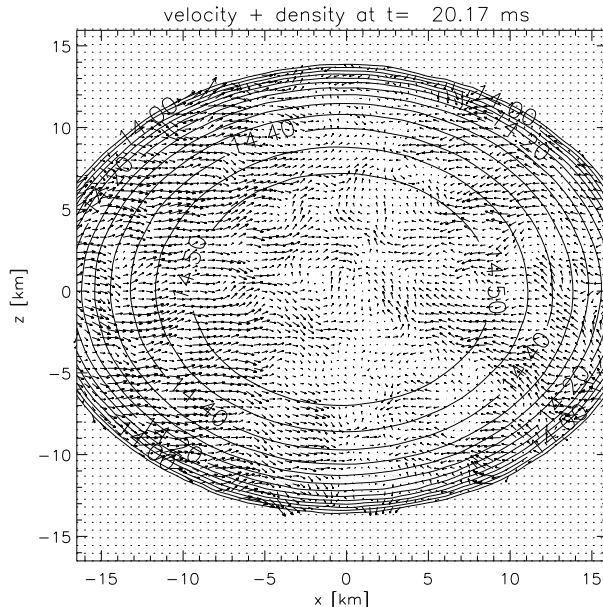


FIGURE 1. Velocity field (space-fixed frame) inside the central object of the remnant of a neutron star coalescence. The labels at the contour lines refer to $\log(\rho)$, typical fluid velocities are $\sim 10^8$ cm/s.

nuclear physics (“exotic” condensates etc.) could influence the results, but estimates of up to many seconds are not unrealistic.

SIMULATIONS

We have performed 3D simulations of the last inspiral stages and the subsequent coalescence for about 20 ms. We use a temperature and composition dependent nuclear equation of state that covers the whole relevant parameter space in density, temperature and composition [21, 14]. In addition, a detailed, multi-flavour neutrino treatment has been applied to account for energy losses and compositional changes due to neutrino processes. The neutrino treatment and the results concerning the neutrino emission have been described in detail in [16]. To solve the hydrodynamic equations we use the smoothed particle hydrodynamics method (SPH), the simulations are performed with up to more than a million SPH particles. We use Newtonian self-gravity plus extra forces emerging from the emission of gravitational waves. The details of the production runs as well as those of several test runs can be found in [14, 16, 17]. Results focusing particularly on gamma-ray bursts have been presented in [15, 17, 18].

DYNAMO ACTION IN MERGER REMNANTS

Before proceeding further with the argumentation, it is worth pointing out that the fluid flow never becomes axisymmetric during the simulation and therefore Cowlings anti-dynamo theorem does not apply here.

The central object of the merger remnant is differentially rapidly rotating with rotation periods below 1 ms over a large fraction of the central object’s radius, examples of rotation profiles can be found in [14]. When the stellar surfaces come into contact, a vortex sheet forms between them across which the tangential velocities exhibit a discontinuity. This vortex sheet is Kelvin-Helmholtz-unstable with the shortest modes growing fastest. These fluid instabilities lead complex flow patterns inside the central object of the merger remnant. In the orbital plane they manifest themselves as strings of vortex rolls that may merge (see Fig. 8 in [14]). An example of the flow pattern perpendicular to the orbital plane is shown in Fig. 1. This pattern caused by fluid instabilities exhibits “cells” of size $l_c \sim 1$ km and velocities of $v_c \sim 10^8$ cm/s.

Moreover, the neutrino optical depth drops very steeply from $\sim 10^4$ at the centre to the edge of the central object (see Fig. 11 in [16]). For this reason the outer layers lose neutrino energy, entropy and lepton number at a much higher rate than the interior, this leads to a gradual build-up of a negative entropy and lepton number gradient which will drive vigorous convection [3, 1]. We expect this to set in after a substantial fraction of the neutrino cooling time (i.e. on time scales longer than our simulated time) when a lot of the thermal energy of the remnant has been radiated away. The situation is comparable to the convection in a new-born protoneutron star, but here we have around twice the mass and the matter is much more deleptonized ($Y_e \sim 0.1$). As both the fluid instabilities and the neutrino-driven convection have very similar properties, we will not further distinguish between them in this context. Assuming neutrinos to be the dominant source of viscosity [22] we estimate a viscous damping time scale of the order $\tau_c \sim l_c^2/\nu_\nu \sim 60$ s, where ν_ν is the neutrino viscosity. In other words the fluid pattern will be damped out only on a time scale that is much longer than the time scales of interest here.

We expect an efficient $\alpha - \Omega$ -dynamo to be at work in the merger remnant. The differential rotation will wind up initial poloidal into a strong toroidal field (“ Ω -effect”), the fluid instabilities/convection will transform toroidal fields into poloidal ones and vice versa (“ α -effect”). Usually, the Rossby number, $Ro \equiv \frac{\tau_{rot}}{\tau_{conv}}$ is adopted as a measure of the efficiency of dynamo action in a star. In the central object we find Rossby numbers well below unity, ~ 0.4 , and therefore expect an efficient amplification of initial seed magnetic fields. A convective dynamo amplifies initial fields exponentially with an e-folding time given approximately by the convective overturn time, $\tau_c \approx 3$ ms; the saturation field strength is thereby independent of the initial seed field (Nordlund et al. 1992).

Adopting the kinematic dynamo approximation we find that, if we start with a typical neutron star magnetic field, $B_0 = 10^{12}$ G, as seed, equipartition field strength in the central object will be reached (provided enough kinetic energy is available, see below) in only ≈ 40 ms. The equipartition field strengths in the remnant are a few times 10^{17} G for the central object and around $\sim 10^{15}$ G for the surrounding torus (see Fig. 8 in [17]). To estimate the maximum obtainable magnetic field strength (averaged over the central object) we assume that all of the available kinetic energy can be transformed into mag-

netic field energy. Using the kinetic energy stored in the rotation of the central object, $E_{\text{kin}} = 8 \cdot 10^{52}$ erg for our generic simulation, we find $\langle B_{co} \rangle = \sqrt{3 \cdot E_{\text{kin}} / R_{co}^3} \approx 3 \cdot 10^{17}$ G (note that if only a fraction of 0.1 of the equipartition pressure should be reached this would still correspond to $\sim 10^{17}$ G).

GAMMA-RAY BURSTS

There are various ways how this huge field strength could be used to produce a GRB. The fields in the vortex rolls (see Fig. 8 in [14]) will wind up the magnetic field fastest. Once they reach field strengths close to the local equipartition value they will become buoyant, float up, break through the surface and possibly reconnect in an ultra-relativistic blast [6]. The time structure imprinted on the sequence of such blasts would then reflect the activity of the fluid instabilities inside the central object. The expected lightcurve of the GRB would therefore be an erratic sequence of sub-bursts with variations on millisecond time scales.

Simultaneously such an object can act as a scaled-up “super-pulsar” and drive out an ultra-relativistic wind. A similar configuration, a millisecond pulsar with a magnetic field of a few times 10^{15} G, formed for example in an accretion-induced collapse, has been suggested as a GRB-model by Usov (1992, 1994). The kinetic energy from the braking of the central object is mainly transformed into magnetic field energy that is frozen in the outflowing plasma. At some stage the plasma becomes transparent to its own photons producing a blackbody component. Further out from the remnant the MHD-approximation breaks down and intense electromagnetic waves of the rotation frequency of the central engine are produced. These will transfer their energy partly into accelerating outflowing particles to Lorentz-factors in excess of 10^6 that can produce an afterglow via interaction with the external medium. The other part goes into non-thermal synchro-Compton radiation with typical energies of ~ 1 MeV [24].

SUMMARY

We have discussed the possibility of dynamo action in the central object created in a neutron star merger, which is expected to be stabilised against gravitational collapse via differential rotation. If it remains so for a good fraction of a second then the initial neutron star magnetic fields are expected to be amplified by a low-Rossby number $\alpha - \Omega$ -dynamo. In principle enough rotational energy is available to attain an average field strength in the central object of $3 \cdot 10^{17}$ G. Locally the equipartition field strength (ranging from 10^{16} to a few times 10^{17} G depending on the exact position in the remnant) may be reached. This will cause the corresponding fluid parcels to float up and produce via reconnection an erratic sequence of ultra-relativistic blasts. In addition the central object can act as a “super-pulsar” of $\sim 10^{17}$ G that transforms most of its rotational energy into an ultra-relativistic wind with frozen-in magnetic field. As shown in [24] such a wind will result in a black-body component plus synchro-Compton radiation. Such a super-pulsar will spin-down in ~ 0.2 s, just the typical duration of a short GRB.

We have only discussed magnetic processes in the central object of the remnant, but very similar processes are expected from the surrounding torus [9]. Here, however, longer time scales and lower magnetic field strengths are expected, the equipartition fields being around 10^{15} G.

ACKNOWLEDGMENTS

The reported simulations have been performed using the UK Astrophysical Fluids Facility (UKAFF) and the supercomputer of the Mathematical Modelling Centre of the University of Leicester (HEX).

REFERENCES

1. Burrows, A. and Lattimer, J.M., *Phys. Rep.*, 163, 51 (1988)
2. Duncan, R.C. and Thompson, C., *ApJ*, 392, L9 (1992)
3. Epstein, R.I., *MNRAS*, 188, 305 (1979)
4. Faber, J.A., Rasio, F.A. and Manor, J.B., *Phys.Rev. D*63, 044012(2001)
5. Katz, J.I., *ApJ*, 490, 633 (1997)
6. Kluzniak, W.; Ruderman, M., *ApJ*, 505, L113 (1998)
7. Lyford, N. D., Baumgarte, T.W. and Shapiro, Stuart L., *ApJ*, 583, L410 (2002)
8. Meszaros, P. and Rees, M.J., *ApJ*, 482, L29 (1997)
9. Narayan, R., Paczynski, B. and Piran, T., *ApJ*, 395, L83 (1992)
10. Nordlund et al., *ApJ*, 392, 647 (1992)
11. Ostriker, P. and Bodenheimer, J.P., *ApJ*, 151, 1089 (1968)
12. Rasio, F.A. and Shapiro, S.L., *Class.Quant.Grav.* 16, R1-R29 (1999)
13. Rosswog, S.; Liebendörfer, M.; Thielemann, F.-K.; Davies, M. B.; Benz, W.; Piran, T., *A&A*, 341, 400 (1999)
14. S. Rosswog, M.B. Davies, *MNRAS*, **334**, 481 (2002)
15. S. Rosswog, E. Ramirez-Ruiz, *MNRAS*, **336**, L7 (2002)
16. S. Rosswog, M. Liebendörfer, *MNRAS*, 342, 673 (2003)
17. S. Rosswog, E. Ramirez-Ruiz, *MNRAS*, 343, L36 (2003)
18. S. Rosswog, E. Ramirez-Ruiz, M.B. Davies, *MNRAS*, 345, 1077 (2003)
19. Ruffert M., Janka H.-T., Schäfer G., 1996, *A & A*, 311, 532
20. Ruffert M., Janka H.-T., Takahashi K., Schäfer G., 1997, *A & A*, 319, 122
21. Shen H., Toki H., Oyamatsu K., Sumiyoshi K., *Nuclear Physics, A* **637**, 435 (1998); Shen H., Toki H., Oyamatsu K., Sumiyoshi K., *Prog. Theor. Phys.*, **100**, 1013 (1998)
22. Thompson, C. & Duncan, R.C., *ApJ*, 408, 194 (1993)
23. Usov, V.V., *Nature*, 357, 472 (1992)
24. Usov, V.V., *MNRAS*, 267, 1035 (1994)